

# A parent Hubbard model for spin-1 Haldane chains

G. Catarina<sup>1,2,3,\*</sup>, J. Fernández-Rossier<sup>1,†</sup>

<sup>1</sup>*QuantaLab, International Iberian Nanotechnology Laboratory (INL), 4715-330 Braga, Portugal*

<sup>2</sup>*Departamento de Física Aplicada, Universidad de Alicante, 03690 San Vicente del Raspeig, Spain and*

<sup>3</sup>*Centro de Física das Universidades do Minho e do Porto, Universidade do Minho, Campus de Gualtar, 4710-057 Braga, Portugal*

(Dated: October 15, 2021)

The Haldane phase for antiferromagnetic spin-1 chains is a celebrated topological state of matter, featuring gapped excitations and fractional spin-1/2 edge states. Here we provide numerical evidence that this phase can be realized with a Hubbard model at half-filling, where each  $s = 1$  spin is stored in a four-site fermionic structure. We find that the noninteracting limit of our proposed parent model describes a one-dimensional topological insulator, adiabatically connected to the Haldane phase. Our work suggests a route to build spin-1 networks using Hubbard model quantum simulators.

The emergence of physical properties that are absent in the building blocks of interacting quantum systems is a central theme of condensed matter physics. Fractionalization, a phenomenon whereby the collective excitations of a system have quantum numbers that cannot be obtained from its elementary constituents, provides a powerful evidence of the *more is different* paradigm [1].

One of the simplest models that features fractionalization is the Heisenberg Hamiltonian for spin-1 chains with nearest-neighbor antiferromagnetic (AF) interactions  $\hat{\mathbf{S}}_i \cdot \hat{\mathbf{S}}_{i+1}$  (where  $\hat{\mathbf{S}}_i$  denotes the vector of spin-1 operators at site  $i$ ). In contrast to the spin-1/2 counterparts, Haldane predicted [2, 3] that one-dimensional (1D) spin-1 Heisenberg antiferromagnets with *periodic boundary conditions* should have a gapped excitation spectrum, along with a singlet ground state for which the spin-spin correlation function decays exponentially.

The seminal work of Haldane was later backed up by the analytical valence bond solid solution of the Affleck–Kennedy–Lieb–Tasaki (AKLT) model [4], where Haldane’s conjecture was rigorously verified for the 1D AF spin-1 Heisenberg Hamiltonian with additional nearest-neighbor biquadratic terms  $\beta(\hat{\mathbf{S}}_i \cdot \hat{\mathbf{S}}_{i+1})^2$ , taking  $\beta = 1/3$ . Remarkably, the AKLT solution for *open boundary conditions* revealed a fourfold degenerate ground state due to the emergence of two fractional spin-1/2 degrees of freedom at the chain edges.

Further numerical work [5, 6] established that the generalization of the AKLT Hamiltonian for arbitrary  $\beta$ , hereafter referred to as the bilinear-biquadratic (BLBQ) model, features both the gapped excitations and the fractional spin-1/2 edge states, with a fourfold degeneracy in the thermodynamic limit, in a range of  $\beta$  that includes  $0 \leq \beta \leq 1/3$ . We refer to this as the Haldane phase.

The connection between the nature of the boundary

conditions and the ground state degeneracy is a hallmark of topological order. In the case of spin-1 Haldane chains, it has been shown that a hidden form of topological AF order, akin to that of the fractional quantum Hall effect [7] and intimately related to a symmetry breaking [8], can be detected through nonlocal string order parameters [9, 10]. It is now understood that the Haldane phase is a symmetry-protected topological phase [11, 12].

In this manuscript, we present a *parent* Hubbard model that captures the Haldane physics of spin-1 BLBQ chains. We consider a Hubbard Hamiltonian at half-filling, defined in a 1D lattice with four sites per unit cell, and show, by numerical means, that its low-energy properties are well described by a BLBQ model in the Haldane phase, thereby connecting two celebrated milestones [13–15] of the last half-century. Furthermore, we find that our proposed parent Hamiltonian interpolates between a spin-1 Haldane chain for  $U > 0$  (where  $U$  denotes the on-site Hubbard repulsion) and a 1D topological insulator in the noninteracting limit  $U = 0$ .

Early work showed that the Haldane phase can be obtained in spin-1/2 Heisenberg alternating chains [16] and ladders [17, 18] with all couplings of the AF type. Given that, in the limit of large  $U$ , the Hubbard model at half-filling is known to map into a spin-1/2 AF Heisenberg Hamiltonian [19], this opens a way to realize the Haldane physics with Fermi-Hubbard systems [20]. It must also be noted that, by turning off the interactions of a variety of fermionic models in the Haldane phase, both trivial [21, 22] and topological [23, 24] 1D band insulators have been adiabatically retrieved. In contrast to the aforementioned literature, here we put forward a Hubbard Hamiltonian that exhibits fractional spin-1/2 edge states supported in four-site fermionic structures that are robust  $s = 1$  spins, effectively generated for any  $U > 0$  without the need of additional terms.

The first key step of our strategy to realize the Haldane physics with a Hubbard model is to generate a robust  $s = 1$  spin. Inspired by previous work [25, 26], we propose the *four-site cluster*—a fermionic structure with trigonal planar geometry in which the three outer sites

\*goncalo.catarina@inl.int

†On permanent leave from Departamento de Física Aplicada, Universidad de Alicante, 03690 San Vicente del Raspeig, Spain

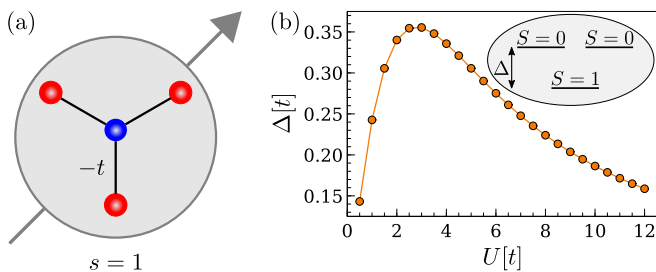


FIG. 1: Four-site cluster as a robust spin-1 building block. (a) Representation of a four-site cluster as an  $s = 1$  spin. Colors of small circles denote the two sublattices. (b) Energy splitting between the  $S = 1$  ground state and the first excited state, as a function of  $U$ , obtained with the Hubbard model for the four-site cluster at half-filling.

are linked to the central one via an intracluster hopping  $t > 0$  (Fig. 1a). The four-site cluster is bipartite and has a sublattice imbalance of  $|N_A - N_B| = 2$  (where  $N_{A/B}$  denotes the number of sites of the  $A/B$  sublattice) which implies, by virtue of Lieb’s theorem [27], that the corresponding Hubbard model at half-filling must yield a ground state with total spin  $S = 1$ . Moreover, exact diagonalization of the model yields a splitting  $\Delta$  between the  $S = 1$  ground state and a doublet of  $S = 0$  first excited states (Fig. 1b) that is at least one order of magnitude larger than the effective exchange coupling  $J$  computed below. Previous work has shown that this splitting is maximal, compared to other  $|N_A - N_B| = 2$  structures, due to its  $C_3$  symmetry [25]. Therefore, we establish the four-site cluster as our robust spin-1 building block, mapping four fermionic sites into one  $s = 1$  spin.

The next step toward the realization of the Haldane phase is to create a 1D lattice of antiferromagnetically coupled  $s = 1$  four-site clusters. We first consider the case of  $N = 2$  chains (where  $N$  denotes either the number of four-site clusters or the number of  $s = 1$  spins), which we refer to as *dimers*. To achieve an effective AF coupling in the four-site dimer, we introduce an intercluster hopping  $t' > 0$  between the closest sites of each of the two four-site clusters (Fig. 2a). We find that, for small enough  $t'$ —which preserves the picture of robust spin-1 building blocks (see the Supplemental Material for technical details on how the upper bounds of  $t'$  are set)—, the four-site Hubbard dimer at half-filling yields a low-energy spectrum that can be matched, spin degeneracies included, to that of the BLBQ model with an effective AF exchange coupling  $J > 0$ ,

$$\hat{H}_{\text{BLBQ}} = J \sum_{i=1}^{N-1} \left[ \hat{\mathbf{S}}_i \cdot \hat{\mathbf{S}}_{i+1} + \beta \left( \hat{\mathbf{S}}_i \cdot \hat{\mathbf{S}}_{i+1} \right)^2 \right], \quad (1)$$

for  $N = 2$ , thereby establishing a mapping between four-site Hubbard and spin-1 BLBQ dimers (Fig. 2a). It must be noted that a small but nonzero biquadratic exchange coupling—the simplest term that can be added to  $N = 2$

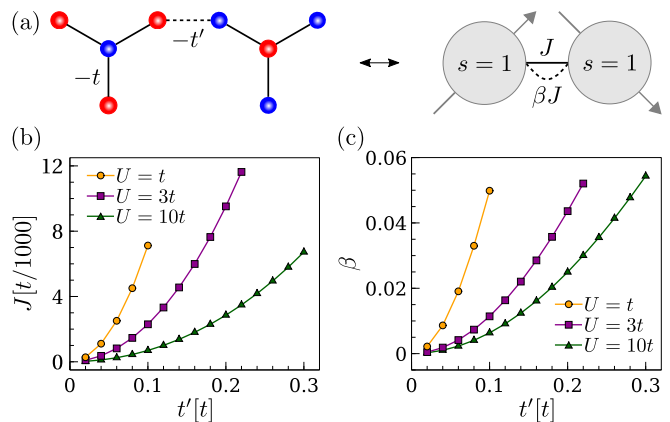


FIG. 2: Effective spin picture of two coupled four-site clusters. (a) Depiction of a four-site dimer as an AF spin-1 dimer with bilinear ( $J$ ) and biquadratic ( $\beta J$ ) exchange couplings. (b,c) BLBQ model parameters  $J$  (b) and  $\beta$  (c), as a function of the Hubbard model parameters, obtained by matching the energy levels of the spin-1 BLBQ dimer to the low-energy spectrum of the four-site Hubbard dimer at half-filling.

Heisenberg chains, compatible with all the symmetries of the system—is necessary to obtain an exact match.

Figure 2b,c shows the BLBQ model parameters  $J$  (Fig. 2b) and  $\beta$  (Fig. 2c), as a function of the Hubbard model parameters, obtained by fitting the energy levels of the spin-1 BLBQ dimer, solved analytically, to the low-energy spectrum of the four-site Hubbard dimer at half-filling, solved by exact diagonalization. We highlight three main features. First, we note that  $J$  is at least one order of magnitude smaller than  $\Delta$ , as previously anticipated. This ascertains that the four-site clusters, albeit coupling antiferromagnetically, have a large effective intracluster ferromagnetic exchange that preserves their spin-1 character [52]. Second, we verify that  $J$  follows the superexchange scaling [19]  $J \propto t'^2/U$ . Third, we obtain values of  $\beta$  between 0 and 0.06, in which case the BLBQ model is known to remain in the Haldane phase [5, 6].

To provide further evidence that our proposed 1D four-site Hubbard lattice at half-filling captures the Haldane physics of spin-1 BLBQ chains, we now extend the comparison between both models for chains with  $N > 2$  (Fig. 3a), keeping the same  $J$  and  $\beta$  as obtained for the dimer. We use the QuSpin package [28, 29] to perform exact diagonalization on spin-1 BLBQ chains up to  $N = 19$  (the limit within our computational resources), and the ITensor library [30] for density matrix renormalization group [31, 32] calculations on  $N \geq 20$  spin-1 BLBQ chains and  $N \geq 3$  four-site Hubbard lattices.

Figure 3b-d shows the five lowest energy levels obtained with both Hubbard and BLBQ models for  $N = 10$  chains, using different sets of model parameters. An overall good agreement is apparent, with differences verified to be smaller than  $J/10$  for all the energy levels. We also observe that, whereas the pattern of spin degenera-

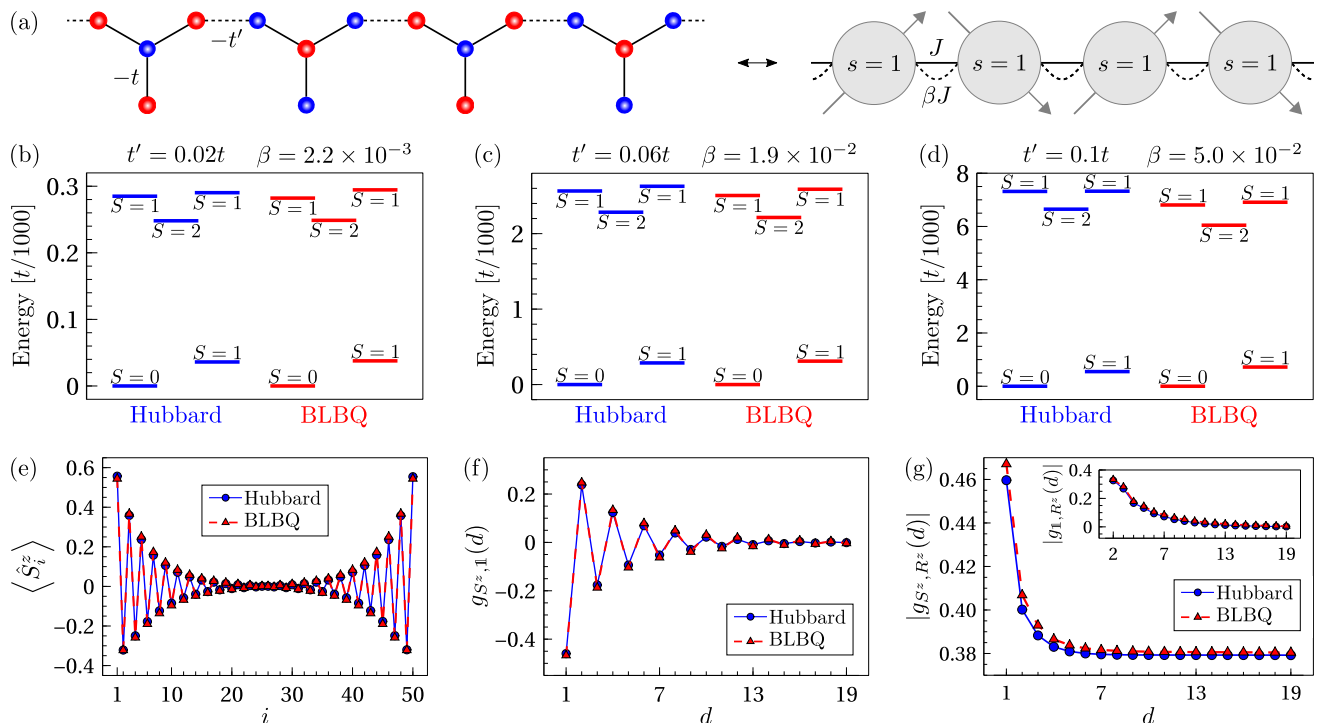


FIG. 3: Agreement of the effective spin-1 model for 1D four-site Hubbard lattices and observation of Haldane phase properties. (a) Sketch of the general mapping between four-site 1D lattices and spin-1 BLBQ chains. (b–d) Comparison between the lowest energy levels of  $N = 10$  four-site Hubbard and spin-1 BLBQ chains. Hubbard model results were obtained at half-filling, for  $U = t$ , with  $t' = 0.02t$  (b),  $t' = 0.06t$  (c), and  $t' = 0.1t$  (d). BLBQ model parameters  $J = 2.8 \times 10^{-4}t$ ,  $\beta = 2.2 \times 10^{-3}$  (b),  $J = 2.5 \times 10^{-3}t$ ,  $\beta = 1.9 \times 10^{-2}$  (c), and  $J = 7.1 \times 10^{-3}t$ ,  $\beta = 5.0 \times 10^{-2}$  (d) were fixed by matching the low-energy spectra of the dimers. Energy levels were shifted as to set the ground state energies to zero. (e–g) Average magnetization (e), spin-spin correlation function (f), and string order parameters (g), obtained for the lowest energy state with  $|S, S_z\rangle = |1, +1\rangle$  of  $N = 50$  four-site Hubbard and spin-1 BLBQ chains, using the same model parameters as in (c).

cies is the same no matter the model parameters taken, the agreement between the energies is worse when  $\beta$  is larger. This suggests that higher-order corrections, such as bicubic exchange couplings, should be included if a better quantitative description is sought.

Now that the low-energy spectra of both Hubbard and BLBQ models was shown to hold a good agreement, we move on to the comparison of other wave function properties. For that matter, we define the correlator

$$g_{\mathcal{O}, \mathcal{U}}(d) = \left\langle \hat{\mathcal{O}}_p \left( \prod_{q=p+1}^{p+d-1} \hat{\mathcal{U}}_q \right) \hat{\mathcal{O}}_{p+d} \right\rangle, \quad (2)$$

where  $\hat{\mathcal{O}}_p$  and  $\hat{\mathcal{U}}_p$  are arbitrary local operators that act on site  $p$ , assumed to be sufficiently away from the edges, so that  $g_{\mathcal{O}, \mathcal{U}}(d)$  is independent of  $p$ . Notably, the spin-string correlator  $|g^{S_z, R^z}(d)|$ , where  $\hat{R}_p^z = \exp(i\pi \hat{S}_p^z)$ , is known to be an order parameter that, when evaluated for a state in the fourfold ground state manifold of spin-1 Haldane chains, converges to a finite value [9] ( $|g^{S_z, R^z}(\infty)| \simeq 0.37$  in the case of the Heisenberg model [6]). On the other hand, the pure-string correlator  $|g_{\uparrow, R^z}(d)|$  has been established as an order parameter that, for the same state,

exhibits the opposite behavior, vanishing in the  $d \gg 1$  limit [10]. For comparison purposes, given that each four-site cluster is mapped into an  $s = 1$  spin, in the case of the Hubbard model we take the local spin operators as the sum of fermionic spin operators over the corresponding four-site clusters, i.e.,

$$\hat{S}_i = \frac{1}{2} \sum_{j \in \text{cluster}_i} \left( \hat{c}_{j, \uparrow}^\dagger \hat{c}_{j, \downarrow}^\dagger \right) \cdot \boldsymbol{\tau} \cdot \begin{pmatrix} \hat{c}_{j, \uparrow} \\ \hat{c}_{j, \downarrow} \end{pmatrix}, \quad (3)$$

where  $\boldsymbol{\tau}$  is the vector of Pauli matrices and  $\hat{c}_{j, \sigma}^\dagger$  ( $\hat{c}_{j, \sigma}$ ) is the creation (annihilation) operator for an electron in site  $j$  with spin  $\sigma = \uparrow, \downarrow$ .

In Fig. 3e–g, we present expectation values and correlators computed for the lowest energy state with  $|S, S_z\rangle = |1, +1\rangle$  (where  $S_z$  denotes the total spin projection) of  $N = 50$  chains, using both Hubbard and BLBQ models. Figure 3e shows the average magnetization, which features the well-known signature [32] of spin-1/2 edge fractionalization. In Fig. 3f, we plot the spin-spin correlation function  $g^{S_z, \uparrow}(d) = \langle \hat{S}_p^z \hat{S}_{p+d}^z \rangle$ , which exhibits AF correlations that decay exponentially in the bulk, as expected in the Haldane phase due to the absence of long-range order [2]. Figure 3g provides the ultimate evidence that

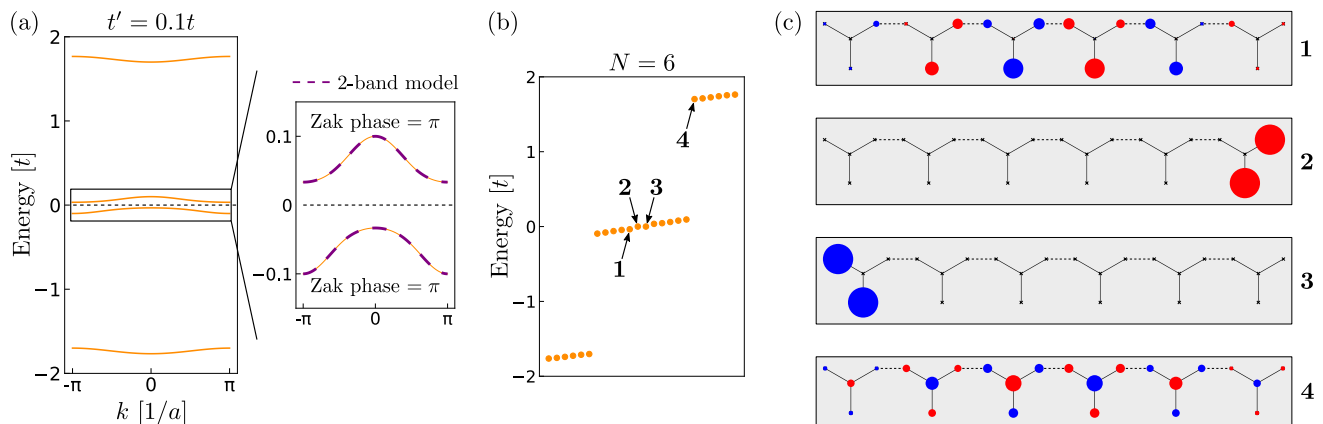


FIG. 4: Topology of the four-site 1D lattice in the noninteracting limit. (a) Energy bands of the four-site 1D crystal, obtained with the tight-binding model for  $t' = 0.1t$ . Horizontal dashed line marks the Fermi level at half-filling. The low-energy bands feature a gap, along with a topological Zak phase of  $\pi$ , and are well described by an effective two-band model obtained for  $t' \ll t$ . (b,c) Energy levels (b) and atomic wave function distribution of the marked eigenstates (c), obtained with the tight-binding model for an  $N = 6$  four-site lattice with  $t' = 0.1t$ . Colors and size of the circles in (c) represent the two sublattices and the wave function overlap at each site, respectively. The eigenstates at half-filling (**2** and **3**) are zero-energy states localized at the edges. All other eigenstates have nonzero energy and bulk character (**1** and **4** are shown as examples).

both models capture the Haldane physics, as the string order parameters  $|g_{S^z, R^z}(d)|$  and  $|g_{\mathbf{1}, R^z}(d)|$  are shown to follow the characteristic behaviors [9, 10]. Notably, both models yield a striking agreement in all these calculations, thus supporting our claim of its equivalence.

For completeness, we have verified that the Hubbard-BLBQ mapping holds not only for  $U = t$  (Fig. 3), but for all  $U > 0$ . In the Supplemental Material, we show calculations for  $U = 0.1t$ , relevant to connect with the noninteracting limit, and for  $U = 10t$ , in which case the Hubbard model effectively maps into a spin-1/2 Heisenberg Hamiltonian [19]. It must be noted that the magnitude of  $U$  determines the spin-1 robustness of the four-site clusters (quantified by  $\Delta$ ), with the main consequence being that a maximal  $\Delta$  allows for a maximal  $J$ , a scenario that occurs for  $U \simeq 3t$  (Fig. 1b) [53]. Besides that, in the Supplemental Material we also show that the  $C_3$  symmetry of the four-site clusters is not a necessary requirement for the Hubbard-BLBQ mapping to hold.

We now consider the  $U = 0$  limit of the four-site 1D lattice. As in the interacting case, we take  $t' \ll t$ . Figure 4a shows the energy bands of the four-site 1D crystal ( $N \rightarrow \infty$ ), which feature a gap at half-filling. We find that the low-energy bands possess a Zak phase of  $\pi$  [54], known to be a topological marker for 1D insulators with inversion symmetry [33]. Expectedly [34], we also find that chains with finite length host two in-gap states localized at the edges (Fig. 4b,c). Interestingly, these states have rigorously zero-energy regardless of  $N$  (Fig. 4b) [55] and are strictly localized at two edge sites (Fig. 4c), in contrast, for instance, to the topological edge states of the Su-Schrieffer-Heeger model [35]. We associate the zero-energy states obtained with our model to a symmetry that consists in interchanging the two dangling sites

of each edge [36].

Finally, we conjecture a topological equivalence between the  $U = 0$  limit of the four-site 1D lattice at half-filling, shown to describe a topological insulator, and the  $U > 0$  regime, that realizes the Haldane symmetry-protected topological phase, according to our computations. Our conjecture is based on two points. First, in both cases the ground state is unique for periodic boundary conditions and degenerate for open-ended chains. Second, Hubbard interactions are not expected to close the  $U = 0$  gap and therefore it is possible to adiabatically deform the  $U = 0$  limit into the  $U > 0$  regime.

In conclusion, we have shown that a Hubbard Hamiltonian at half-filling, defined in a 1D lattice that hosts effective  $s = 1$  spins at each of its four-site unit cells, realizes the Haldane phase. The proposed strategy opens a way to engineer spin-1 Haldane chains, as well as other layouts, through a variety of physical systems that are being explored for quantum simulation of the Hubbard model, such as cold atoms [37, 38], quantum dots [39, 40], dopant arrays [41], hydrogenated graphene bilayers [42] and spin-1/2 networks [43, 44]. Our findings pave the way to new experiments, going beyond early seminal works [45–47], as well as the recent observations on triangulene spin chains [26]. Additional interest comes from the fact that both the AKLT ground state and its spin-3/2 counterpart on a honeycomb lattice are resources for measurement-based quantum computing [48, 49].

We thank R. Ortiz and J. L. Lado for fruitful discussions, and J. C. Sancho-García for access to computer facilities. We acknowledge financial support from the Portuguese FCT (Grant No. SFRH/BD/138806/2018), MINECO-Spain (Grant No. PID2019-109539GB-41) and Generalitat Valenciana (Grant No. Prometeo2017/139).

- 
- [1] P. W. Anderson, *Science* **177**, 393 (1972).
- [2] F. D. M. Haldane, *Physics Letters A* **93**, 464 (1983).
- [3] F. D. M. Haldane, *Phys. Rev. Lett.* **50**, 1153 (1983).
- [4] I. Affleck, T. Kennedy, E. H. Lieb, and H. Tasaki, *Phys. Rev. Lett.* **59**, 799 (1987).
- [5] T. Kennedy, *Journal of Physics: Condensed Matter* **2**, 5737 (1990).
- [6] S. R. White and D. A. Huse, *Phys. Rev. B* **48**, 3844 (1993).
- [7] S. M. Girvin and D. P. Arovas, *Physica Scripta* **T27**, 156 (1989).
- [8] T. Kennedy and H. Tasaki, *Phys. Rev. B* **45**, 304 (1992).
- [9] M. den Nijs and K. Rommelse, *Phys. Rev. B* **40**, 4709 (1989).
- [10] F. Pollmann and A. M. Turner, *Phys. Rev. B* **86**, 125441 (2012).
- [11] Z.-C. Gu and X.-G. Wen, *Phys. Rev. B* **80**, 155131 (2009).
- [12] F. Pollmann, A. M. Turner, E. Berg, and M. Oshikawa, *Phys. Rev. B* **81**, 064439 (2010).
- [13] I. Affleck, *Journal of Physics: Condensed Matter* **1**, 3047 (1989).
- [14] H. Tasaki, *Journal of Physics: Condensed Matter* **10**, 4353 (1998).
- [15] D. P. Arovas, E. Berg, S. A. Kivelson, and S. Raghu, (2021), arXiv preprint arXiv:2103.12097.
- [16] K. Hida, *Phys. Rev. B* **45**, 2207 (1992).
- [17] T. Barnes, E. Dagotto, J. Riera, and E. S. Swanson, *Phys. Rev. B* **47**, 3196 (1993).
- [18] S. R. White, *Phys. Rev. B* **53**, 52 (1996).
- [19] P. W. Anderson, *Phys. Rev.* **115**, 2 (1959).
- [20] P. Sompet, S. Hirthe, D. Bourgund, T. Chalopin, J. Bibo, J. Koepsell, P. Bojović, R. Verresen, F. Pollmann, G. Salomon, C. Gross, T. A. Hilker, and I. Bloch, (2021), arXiv preprint arXiv:2103.10421.
- [21] F. Anfuso and A. Rosch, *Phys. Rev. B* **75**, 144420 (2007).
- [22] S. Moudgalya and F. Pollmann, *Phys. Rev. B* **91**, 155128 (2015).
- [23] F. T. Lisandrini, A. M. Lobos, A. O. Dobry, and C. J. Gazza, *Phys. Rev. B* **96**, 075124 (2017).
- [24] M. R. Zirnbauer, *Journal of Mathematical Physics* **62**, 021101 (2021).
- [25] R. Ortiz, R. A. Boto, N. García-Martínez, J. C. Sancho-García, M. Melle-Franco, and J. Fernández-Rossier, *Nano Letters* **19**, 5991 (2019).
- [26] S. Mishra, G. Catarina, F. Wu, R. Ortiz, D. Jacob, K. Eimre, J. Ma, C. A. Pignedoli, X. Feng, P. Ruffieux, J. Fernández-Rossier, and R. Fasel, *Nature* **598**, 287 (2021).
- [27] E. H. Lieb, *Phys. Rev. Lett.* **62**, 1201 (1989).
- [28] P. Weinberg and M. Bukov, *SciPost Phys.* **2**, 003 (2017).
- [29] P. Weinberg and M. Bukov, *SciPost Phys.* **7**, 20 (2019).
- [30] M. Fishman, S. R. White, and E. M. Stoudenmire, *The ITensor software library for tensor network calculations* (2020), arXiv preprint arXiv:2007.14822.
- [31] S. R. White, *Phys. Rev. Lett.* **69**, 2863 (1992).
- [32] S. R. White, *Phys. Rev. B* **48**, 10345 (1993).
- [33] J. Zak, *Phys. Rev. Lett.* **62**, 2747 (1989).
- [34] P. Delplace, D. Ullmo, and G. Montambaux, *Phys. Rev. B* **84**, 195452 (2011).
- [35] W. P. Su, J. R. Schrieffer, and A. J. Heeger, *Phys. Rev. Lett.* **42**, 1698 (1979).
- [36] M. Koshino, T. Morimoto, and M. Sato, *Phys. Rev. B* **90**, 115207 (2014).
- [37] S. Murmann, A. Bergschneider, V. M. Klinkhamer, G. Zürn, T. Lompe, and S. Jochim, *Phys. Rev. Lett.* **114**, 080402 (2015).
- [38] A. Mazurenko, C. S. Chiu, G. Ji, M. F. Parsons, M. Kanász-Nagy, R. Schmidt, F. Grusdt, E. Demler, D. Greif, and M. Greiner, *Nature* **545**, 462 (2017).
- [39] T. Hensgens, T. Fujita, L. Janssen, X. Li, C. J. Van Diepen, C. Reichl, W. Wegscheider, S. Das Sarma, and L. M. K. Vandersypen, *Nature* **548**, 70 (2017).
- [40] P.-A. Mortemousque, E. Chanrion, B. Jadot, H. Flentje, A. Ludwig, A. D. Wieck, M. Urdampilleta, C. Bäuerle, and T. Meunier, *Nature Nanotechnology* **16**, 296 (2021).
- [41] J. Salfi, J. A. Mol, R. Rahman, G. Klimeck, M. Y. Simmons, L. C. L. Hollenberg, and S. Rogge, *Nature Communications* **7**, 11342 (2016).
- [42] N. A. García-Martínez and J. Fernández-Rossier, *Phys. Rev. Research* **1**, 033173 (2019).
- [43] K. Yang, Y. Bae, W. Paul, F. D. Natterer, P. Willke, J. L. Lado, A. Ferrón, T. Choi, J. Fernández-Rossier, A. J. Heinrich, and C. P. Lutz, *Phys. Rev. Lett.* **119**, 227206 (2017).
- [44] K. Yang, S.-H. Phark, Y. Bae, T. Esat, P. Willke, A. Ardavan, A. J. Heinrich, and C. P. Lutz, *Nature Communications* **12**, 993 (2021).
- [45] W. J. L. Buyers, R. M. Morra, R. L. Armstrong, M. J. Hogan, P. Gerlach, Hirakawa, and K., *Phys. Rev. Lett.* **56**, 371 (1986).
- [46] J. P. Renard, M. Verdaguer, L. P. Regnault, W. A. C. Erkelens, J. Rossat-Mignod, and W. G. Stirling, *EPL (Europhysics Letters)* **3**, 945 (1987).
- [47] M. Hagiwara, K. Katsumata, I. Affleck, B. I. Halperin, and J. P. Renard, *Phys. Rev. Lett.* **65**, 3181 (1990).
- [48] T.-C. Wei, I. Affleck, and R. Raussendorf, *Phys. Rev. Lett.* **106**, 070501 (2011).
- [49] T.-C. Wei, I. Affleck, and R. Raussendorf, *Phys. Rev. A* **86**, 032328 (2012).
- [50] S. Mishra, D. Beyer, K. Eimre, R. Ortiz, J. Fernández-Rossier, R. Berger, O. Gröning, C. A. Pignedoli, R. Fasel, X. Feng, and P. Ruffieux, *Angewandte Chemie International Edition* **59**, 12041 (2020).
- [51] B. Sutherland, *Phys. Rev. B* **34**, 5208 (1986).
- [52] A similar picture has been reported in triangulene dimers [50], where each triangulene plays the role of the effective  $s = 1$  spin.
- [53] Note that, even though  $J$  scales as  $J \propto t'^2/U$ , a smaller  $U$  does not necessarily imply a larger  $J$  since the upper bounds of  $t'$  for which the Hubbard-BLBQ mapping remains valid also depend on  $U$ .
- [54] See the Supplemental Material for the derivation of an effective two-band model from which this result can be obtained analytically.
- [55] Note that, for even  $N$ ,  $N_A = N_B$  and Sutherland's theorem [51] does not warrant the presence of zero-energy states.